

# CrystEngComm

Accepted Manuscript



This is an *Accepted Manuscript*, which has been through the Royal Society of Chemistry peer review process and has been accepted for publication.

*Accepted Manuscripts* are published online shortly after acceptance, before technical editing, formatting and proof reading. Using this free service, authors can make their results available to the community, in citable form, before we publish the edited article. We will replace this *Accepted Manuscript* with the edited and formatted *Advance Article* as soon as it is available.

You can find more information about *Accepted Manuscripts* in the [Information for Authors](#).

Please note that technical editing may introduce minor changes to the text and/or graphics, which may alter content. The journal's standard [Terms & Conditions](#) and the [Ethical guidelines](#) still apply. In no event shall the Royal Society of Chemistry be held responsible for any errors or omissions in this *Accepted Manuscript* or any consequences arising from the use of any information it contains.

## ARTICLE

## Ethanol Gas Sensor Based on Self-Supporting Hierarchical SnO<sub>2</sub> Nanorods Array

Cite this: DOI: 10.1039/x0xx00000x

Qian Liu,<sup>a</sup> Zhenyu Zhang,<sup>a</sup> Wenyao Li,<sup>a,b</sup> Kaibing Xu,<sup>a</sup> Rujia Zou<sup>a,\*</sup> and Junqing Hu<sup>a,\*</sup>Received 00th January 2012,  
Accepted 00th January 2012

DOI: 10.1039/x0xx00000x

www.rsc.org/

3D array nanostructures assembled from 0D nanoparticles, 1D nanorods, nanowires, nanotubes, and 2D nanosheets on specific substrates are an important class of architecture in nanomaterials application. SnO<sub>2</sub> nanostructures arrays on different kinds of heterogeneous substrates have been reported. Here, we provide a self-supporting 3D hierarchical SnO<sub>2</sub> nanorods array on homogeneous substrate by one-step solvothermal route with the help of anionic surfactant. By investigating the morphology of products using different reaction conditions, the forming mechanism of the structure is proposed. The self-supporting SnO<sub>2</sub> nanorods array is applied as gas sensor to a series of harmful gases. It exhibited high response (Sr = 22.69) to ethanol gas with a low concentration of 50 ppm at 260 °C. The unique structure of large surface area and interval space accounts for the good performance in gas sensing.

### Introduction

Design of hierarchical nanostructures from low-dimensional nanostructured building blocks in a desired and controlled manner is not only an interesting topic of nanomaterials research, it is also an important route to improve the properties of a nanomaterials. Actually, 3D (three dimensional) array structures assembled from 0D nanoparticles,<sup>1,2</sup> 1D nanorods,<sup>3</sup> nanowires,<sup>4</sup> nanotubes<sup>5</sup> and 2D nanosheets<sup>6</sup> on specific substrates have the merits of large surface area, high porosity, potential for high loading capacity, facilitating the charge transfer and collection, easy access and preferable to fabricating devices.<sup>7,8</sup> These advantages are crucially valuable in the application fields that based on the chemical reaction between materials and surroundings, for example, gas sensing.

As an important wide-bandgap n-type semiconductor, tin dioxide (SnO<sub>2</sub>) has been demonstrated a promising semiconductor material because the excellent performance in gas sensors,<sup>1,2,4,8,9,10</sup> lithium-ion battery (LIB),<sup>11,12,13,14</sup> field emission,<sup>15,16</sup> sensitized solar cells,<sup>17,18</sup> photocatalyst,<sup>19,20</sup> and so on. Specially, good gas sensing properties of SnO<sub>2</sub> is benefit from the high mobility of conducting electrons, and good chemical and thermal stability.<sup>21,22</sup> So far, much effort has been devoted to synthesis of novel nanostructure to satisfy the requirements. High surface-to-volume ratio of nanomaterials was verified to be preferable for the detection of gases.<sup>23</sup> 3D array nanostructures, combining the 1D SnO<sub>2</sub> nanostructures with a substrate, have been demonstrating better performances than the disordered 1D building blocks. For example, SnO<sub>2</sub> nanorod array on graphene substrate synthesized via the "nanocrystal-seeds directing" hydrothermal route have exhibited enhanced gas sensing sensitivity to H<sub>2</sub>S gas.<sup>8</sup> Therefore, 3D SnO<sub>2</sub> nanostructure arrays is one of the most suitable candidates for gas sensing. SnO<sub>2</sub> nanostructures arrays on different kinds of heterogeneous substrates, for instance,

SiO<sub>2</sub>,<sup>24</sup> quartz,<sup>25</sup> TiO<sub>2</sub>,<sup>26</sup> FTO,<sup>27,28</sup> metal,<sup>29</sup> alloy,<sup>7</sup> and graphene,<sup>8</sup> etc., have been designed. However, these substrates have some limits due to the barrier of resistance on the heterogeneous junction, chemical instability, mechanical brittleness, and high cost. So, it is still a tremendous challenge to develop a simple and effective method to realize the structure of SnO<sub>2</sub> nanostructure arrays directly standing on homogeneous substrates, which will overcome the drawbacks or problems associated with the others substrates.

Herein, the homogeneous self-supporting 3D hierarchical SnO<sub>2</sub> nanorods array structures were synthesized by one-step solvothermal route, with the help of anionic surfactant. By controlling the reaction conditions, the forming mechanism of the self-supporting 3D hierarchical SnO<sub>2</sub> nanorods array structure was proposed: the layer substrate of SnO<sub>2</sub> is first formed in the lamellar micelle with the help of surfactant, and SnO<sub>2</sub> nanorods grow on both sides of the substrate to form array structure. This self-supporting SnO<sub>2</sub> nanorods array is applied as gas sensor to a series of harmful gases. It exhibited high response (Sr = 22.69) to ethanol with a low concentration of 50 ppm at 260 °C. The unique structure of large surface area and interval space accounts for their good performance in gas sensing, which is better than other reported SnO<sub>2</sub> based gas sensors, such as SnO<sub>2</sub> nanoparticles, nanorods and nanosheets.

### Experimental section

#### Material synthesis

All chemicals were purchased from Sinopharm Chemical Reagent Co. (Shanghai, China) and were used without further purification. The self-supporting 3D hierarchical SnO<sub>2</sub> nanorods array structures were synthesized by one-step solvothermal route. In a typical synthesis, 0.1 M SnCl<sub>4</sub>•5H<sub>2</sub>O and 1 M NaOH was first dissolved in 5 ml deionized water via

vigorously stir. Then, 0.01 mol (alternative quantity was used in comparative experiment) of anionic surfactant SDS (sodium dodecyl sulfate) was dissolved in a mixed solvent composed of 20 ml n-heptane and 5 ml n-amylalcohol. Subsequently, the two solution was mixed and kept stirring for 30 min, generating a uniformly, steadily existing microemulsion. This mixture was then transferred into a teflon-lined autoclave (50 ml) with a stainless-steel shell, and the reaction system was kept at 220 °C for 24 h (alternative time was used in comparative experiment) and naturally cooled to room temperature. The precipitate was washed with deionized water and pure alcohol several times to remove any possible residues, and then dried at 60 °C for characterization and further use.

### Characterization

Powder X-ray diffraction experiments were conducted by a D/max-2550 PC X-ray diffractometer (Rigaku, Japan). The morphologies and structures of the products were characterized by a field-emission scanning electron microscope (S-4800), and a transmission electron microscope (JEM-2100F).

### Gas sensor fabrication and response test

The gas sensing test was carried out in an HW-30A measuring system (Hanwei Electronics Co. Ltd., PR China). The powder products was first calcined at 400 °C for 2 h, and then mixed with terpineol forming a paste and then coated onto an alumina tube-like substrate with a pair of Au electrodes on each end. A small Ni-Cr alloy coil was placed through the tube as a heater to provide the working temperature. In order to improve the long-term stability of the sensors, the sensors were maintained at a working temperature for 7 days. A stationary state gas distribution method was carried out for gas response testing. Detected gases, such as ethanol, were injected into a test chamber and mixed with air (air humidity: 37%). In the measurement electric circuit, a 1MΩ load resistor was connected in the series with the gas sensors. The circuit voltage was 4.5 V, and the output voltage ( $V_{out}$ ) was the terminal voltage of the load resistor. The working temperature of the sensors was adjusted by varying the heating voltage. In this study, the optimal operating temperature (at which the highest response value was exhibited) was selected to be 260 °C. The resistance of the sensor in air or testing gas was measured by monitoring the  $V_{out}$ . The gas response of the sensor in this paper was defined as  $S_r = R_a/R_g$ , where  $R_a$  and  $R_g$  were the resistance in air and in the test gas, respectively. The response or recovery time was estimated as the time taken for the sensor output to reach 90% of its saturation after applying or switching off the gas in a step function.

### Results and discussions

The self-supporting 3D hierarchical SnO<sub>2</sub> nanorods array structures synthesized by solvothermal route was demonstrated to be high yield and repeatable (shown in supporting information). The low-magnification SEM image in Fig. 1a clearly shows the typical morphology of the as-obtained product, and reveals the large scale uniformity of the hierarchical structures. The area of the structures various in a wide range, down to several hundreds of nm<sup>2</sup> and up to several hundreds of μm<sup>2</sup>. In Fig. 1b, high-magnification SEM images viewed from overhead and laterally (inset) are presented, the slant and dense alignment of the nanorods on both sides of the thin layer substrate are clearly shown. The uniform axial length of the nanorods is approximately 300 nm. And the thickness of layer

substrate is estimated to be 60 nm. Combine the SEM image and HRTEM image of an individual SnO<sub>2</sub> nanorod (Fig. 1c), the diameter of the nanorods was in the range of ~10 nm. It also indicates that the SnO<sub>2</sub> nanorods have a smooth surface and an obtuse angle top but not a flat top. As seen from this image, the lattice fringes of the {-110} have a d-spacing of 0.335 nm, and the growth direction is parallel to [001] crystalline orientation, which agree with the characteristic of tetragonal rutile structure SnO<sub>2</sub> crystal.<sup>3</sup> The XRD pattern, Fig. 1e, reveals the crystal structure and phase purity of the as-grown products. All of the diffraction peaks can be indexed to the tetragonal structure of the SnO<sub>2</sub> material with lattice constants of a = 4.75 and c = 3.20 Å, which agree with the values (a = 4.738 and c = 3.187 Å) of the JCPDS card (41-1445). As there is no peak from other materials in the XRD pattern, the product is concluded to be pure without any impurities, therefore the substrates of the nanorods arrays are also the same SnO<sub>2</sub> crystal.

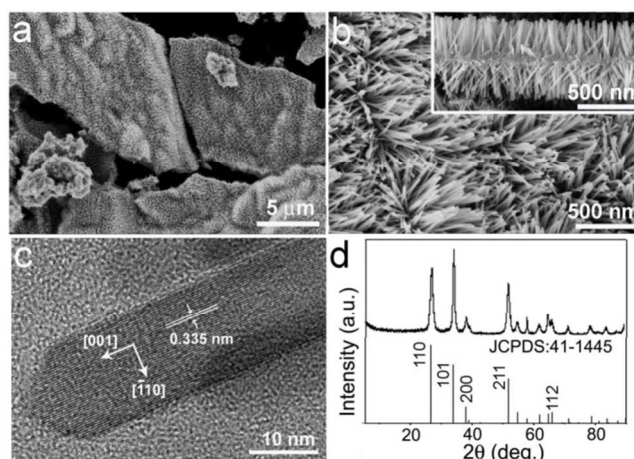


**Fig. 1** (a) and (b) Lower-magnification and higher-magnification SEM image of the as-synthesized self-supporting 3D hierarchical SnO<sub>2</sub> nanorods array, the inset in b is cross section image of the array structure. (c) HRTEM image of SnO<sub>2</sub> nanorod. (d) X-ray diffraction of the as-synthesized self-supporting 3D hierarchical SnO<sub>2</sub> nanorods array sample.

For the purpose of understanding the forming mechanism of this unique self-supporting 3D hierarchical SnO<sub>2</sub> nanorods array structure, systematic investigations were carried out using the SEM images at different reaction conditions. Fig. 2 shows the morphology of the product of SnO<sub>2</sub> heavily depend on the amount of the anionic surfactant SDS. Fig. 2a gives the SEM image of the as-synthesized product without SDS during the solvothermal reaction. The morphology of the SnO<sub>2</sub> product was in random shape and size, other than well-regulated nanostructures. As 0.005 mol of SDS was added into the reaction system, spheres composed of radial SnO<sub>2</sub> nanorods were easily found as revealed in the SEM image, Fig. 2b. The length of the SnO<sub>2</sub> nanorods was estimated to be about 300 nm (according to the diameter of the spheres). In Fig. 2c, the amount of SDS was increased to 0.0075 mol, and some of the SnO<sub>2</sub> nanorods assembled to the array structure. However, not all of the SnO<sub>2</sub> nanorods formed array structure, there are also some nanorods-spheres exist. When the amount of SDS increase to 0.01 mol, almost all the SnO<sub>2</sub> nanorods form array structures on a flat and thin layer substrate, as shown in Fig. 2d. It is concluded that only when the concentration of SDS reach up to a specific level, so called critical micelle concentration (CMC), can the self-supporting 3D hierarchical SnO<sub>2</sub> nanorods array structures form.<sup>30,31</sup>



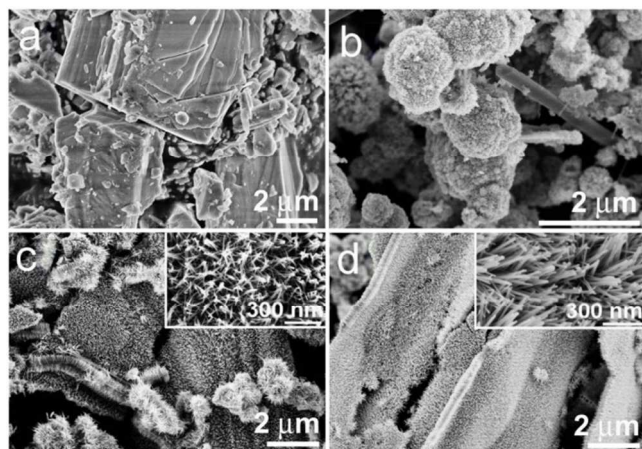


**Fig. 2** SEM images of as-synthesized samples with different amount of SDS used in the preparation, (a) 0 mol, (b) 0.005 mol, (c) 0.0075 mol, and (d) 0.01 mol, respectively.

In order to discover the forming process of the self-supporting 3D hierarchical SnO<sub>2</sub> nanorods array structure, products of various reaction times are selected. Fig. 3 shows a series of SEM images of intermediate products collected from 0.25 h, 3 h, 12 h, and 24 h after the start of solvothermal reaction, respectively. The SEM image shown in Fig. 3a, the SnO<sub>2</sub> nanocrystals assembled to a layer structure. The curled thin layers are tens of nanometers in thick and hundreds of square nanometers in size. As time prolonged, the thin layers are expected to grow larger and thicker, and the flat layer substrate can be formed. Due to the principle of lowest surface free energy during the crystal growth, SnO<sub>2</sub> nanorods can gradually grow longer along the [001] axis as the continuous hydrolysis of Sn<sup>4+</sup> ions. Subsequently, the SnO<sub>2</sub> nanowires grow longer and longer as the increase of the reaction time, till the length up to 300 nm within 24 h, Fig. 3b-d. As revealed in the SEM images, the self-supporting array structure is formed via two steps, and the structure is including the first formed SnO<sub>2</sub> nanocrystal flat layer and then aligned thin SnO<sub>2</sub> nanorods standing on it. Alternatively, the forming process of self-supporting 3D hierarchical SnO<sub>2</sub> nanorods array structure is time dependent.

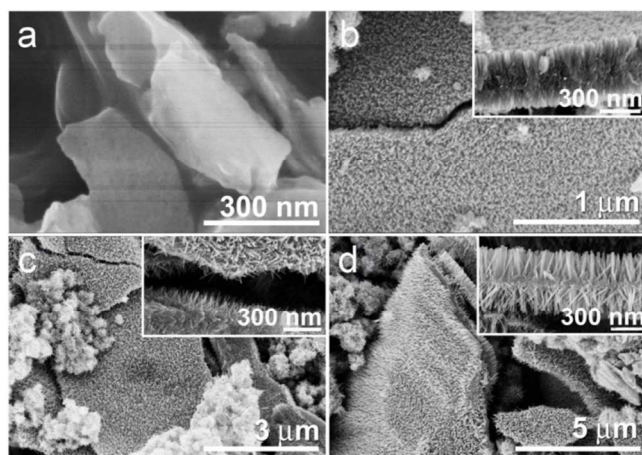


**Fig. 3** SEM images of as-synthesized samples with different reaction duration, (a) 0.25 h, (b) 3 h, (c) 12 h, (d) 24 h, respectively.

On the basis of the experimental results presented above, a reasonable forming mechanism of the self-supporting 3D hierarchical SnO<sub>2</sub> nanorods array structure was proposed. As described in Fig. 4, the SnO<sub>2</sub> nanocrystal thin flat layer structure is first formed, which is heavily depend on the concentration of

surfactant, and then SnO<sub>2</sub> nanorods grew on the self-supporting substrates. The two steps correspond to the nucleation and growth process, respectively. Firstly, due to the liquid reaction environment contains 5 ml deionized water, 20 ml n-heptane and 5 ml n-amylalcohol, water droplets is formed surrounded by oil phase via vigorously stir, Fig. 4a. Then, anionic surfactant SDS, with both hydrophilic and hydrophobic terminals, can form reverse micelles in the water-in-oil system, Fig. 4b. The water droplet is surrounded by the surfactant molecules, hydrophilic terminal is inward and hydrophobic terminal outward. As the concentration of SDS multiplies, the reverse micelles change from globular micelles to lamellar micelles, and exist stably, Fig. 4c. Besides, due to the addition of long chain alcohol, i.e., n-amylalcohol, it is conducive to the formation of lamellar micelles.<sup>32</sup> Therefore, nano-sized water droplets are forced into layered-shape, surrounded by the hydrophilic terminal of SDS molecular. Sn<sup>4+</sup> ion easily hydrolyzes in alkaline solution as described by reaction equation:  $\text{Sn}^{4+} + 6\text{OH}^- \rightarrow \text{Sn}(\text{OH})_6^{2-}$ , and  $\text{Sn}(\text{OH})_6^{2-} \rightarrow \text{SnO}_2 + 2\text{H}_2\text{O} + 2\text{OH}^-$ . Because of the shape of the lamellar micelles, SnO<sub>2</sub> nanocrystallines assembled to be a thin layer, Fig. 4d. In the subsequent solvothermal reaction, the continuously generated Sn(OH)<sub>6</sub><sup>2-</sup> by hydrolysis in the water-oil blending system offered the source for growth of SnO<sub>2</sub> nanorods along the crystal axis [001], Fig. 4e. As reaction time prolong, the nanorods grow longer and longer on both sides of the self-supporting SnO<sub>2</sub> substrate, and leading to the final self-supporting 3D hierarchical SnO<sub>2</sub> nanorods array structure, Fig. 4f.

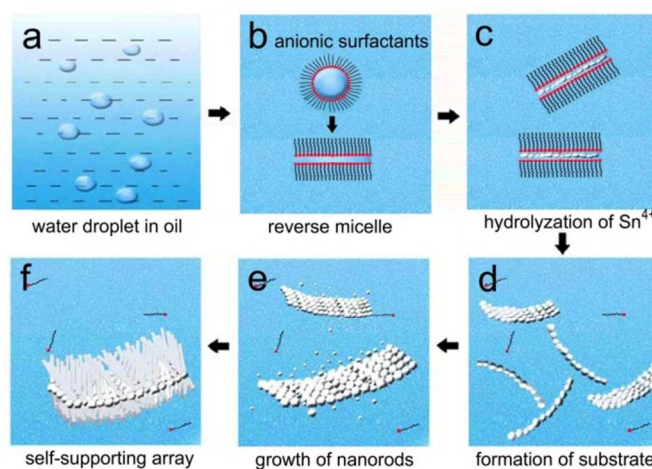


**Fig. 4** (a-f) The formation mechanism diagram of the self-supporting 3D hierarchical SnO<sub>2</sub> nanorods array.

### Gas sensor properties

It is well known that SnO<sub>2</sub> has important practical applications in gas sensing. Attributed to their high-surface-to-volume ratio and ordered arrangement, 3D array structures are preferable for the detection of pollutant gases compared to other individual nanostructures. Therefore, the as-synthesized self-supporting 3D hierarchical SnO<sub>2</sub> nanorods arrays were applied as gas sensors. As indicated in Fig. 5a, it exhibited good response to ethanol with a low concentration of 50 ppm at 260 °C, the response value  $S_r$  is 22.69, which means the resistance of the material in ethanol gas is about 23 times lower than that in atmosphere. That is much higher than the response value in other gases, such as formaldehyde ( $S_r = 8.75$ ) and acetone ( $S_r = 2.05$ ), revealing the selectivity to ethanol. The sensitivity of the SnO<sub>2</sub> nanorods flower structure (Fig. 2b) to 50 ppm ethanol at 260 °C is measured only 5.74, which is much lower than the self-supporting 3D hierarchical SnO<sub>2</sub> nanorods arrays. Fig. 5b shows the dynamic response-recovery curves for self-supporting hierarchical SnO<sub>2</sub>

nanorods arrays at different concentrations of ethanol. Corresponding to various concentrations of 1, 5, 10, 50, 100 ppm cycling test, the response values are 1.54, 3.96, 6.66, 22.69, and 30.12, respectively. This result shows a significant increase compared with SnO<sub>2</sub> nanoparticles<sup>33</sup>, nanorods<sup>34</sup> and nanosheets<sup>35,36</sup>, reported in literatures. As indicated in the cycling curves, the as-synthesized self-supporting 3D hierarchical SnO<sub>2</sub> nanorods arrays reveals fast response and fast recovery to ethanol, the response time and recovery time are 5 s and 2 s, respectively. The concentration detection limit to ethanol gas is as low as of 1 ppm. In the subsequent concentration reduction cycling, as the concentration of ethanol decreased from 100 to 50, 10, 5, 1 ppm, the response values, response and recovery times maintain the same level as former test, demonstrating the stability in service. These results are much better than the reported SnO<sub>2</sub> based gas sensors, such as SnO<sub>2</sub> microspheres<sup>23,37</sup> and nanosheets<sup>35</sup>.

For SnO<sub>2</sub> used as gas sensing materials, the resistance change response to the atmosphere is attributed to the chemical reaction between the reducing gases and the oxygen ions absorbed on the surface of materials, resulting in the release of free electrons.<sup>38</sup> In this case, ethanol (CH<sub>3</sub>CH<sub>2</sub>OH) reacts with the oxygen ions and generated free electrons into the conduction band of SnO<sub>2</sub>, which is expressed as CH<sub>3</sub>CH<sub>2</sub>OH + 6O<sup>-</sup> → 2CO<sub>2</sub> + 3H<sub>2</sub>O + 6e<sup>-</sup>. As it was confirmed that the large surface area and pore size of nanorods arrays are significantly benefit for their gas sensing performance,<sup>8,23</sup> the array structure exactly account for their better performance than the SnO<sub>2</sub> nanorods flower structure as the ethanol sensor. Specifically, the super-thin nanorods and densely aligned SnO<sub>2</sub> nanorods of this self-supporting 3D hierarchical SnO<sub>2</sub> nanorods arrays provide a large surface area, which facilitated the oxygen ions and gas molecular absorption on the surface of material. In addition, the large volume space between the nanorods is benefit to the gas diffusion and mass transport. These are the reasons explaining the good performance in ethanol gas sensing, including high sensitivity, fast response and recovery, and low detection concentration limit.

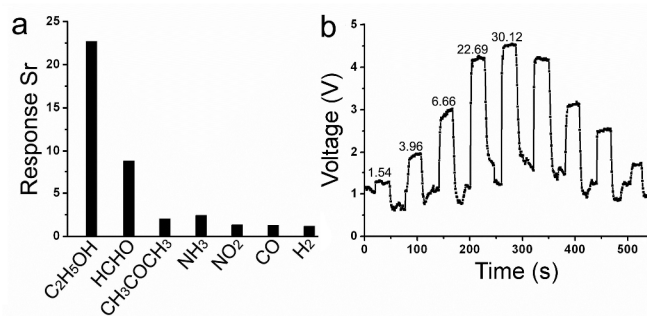


**Fig. 5** (a) The sensitivity ( $S_r$ ) to a series of gases with concentration of 50 ppm. (b) The real-time response curves to a series of ethanol concentration of 1, 5, 10, 50, 100 ppm for the gas sensor made from self-supporting 3D hierarchical SnO<sub>2</sub> nanorods array, and the response value is marked correspondingly.

## Conclusions

In conclusion, self-supporting 3D hierarchical SnO<sub>2</sub> nanorods array structures were synthesized by one-step solvothermal route. The formation process of the novel array structure was investigated, and the forming mechanism was proposed: the SnO<sub>2</sub> nanocrystal thin flat layer structure is first formed, which is heavily depend on the concentration of surfactant, and then SnO<sub>2</sub> nanorods grow on the self-supporting substrates. This unique hierarchical structure of self-supporting SnO<sub>2</sub> nanorods array is applied as gas sensor. It exhibited high response ( $S_r = 22.69$ ) to ethanol with a low concentration of 50

ppm at 260 °C. The unique structure of large surface area and interval space accounts for their good performance in gas sensing. This self-supporting 3D hierarchical SnO<sub>2</sub> nanorods array structure may enrich the class of nanomaterials array structure, and the surfactant-assisted nanomaterial array growth strategy may be extended to other metal oxides.

## Acknowledgements

This work was financially supported by the National Natural Science Foundation of China (Grant Nos. 21171035, 51302035 and 51472049), the Key Grant Project of Chinese Ministry of Education (Grant No. 313015), the PhD Programs Foundation of the Ministry of Education of China (Grant Nos. 20110075110008 and 20130075120001), the National 863 Program of China (Grant No. 2013AA031903), the Science and Technology Commission of Shanghai Municipality (Grant No. 13ZR1451200), the Fundamental Research Funds for the Central Universities, the Program Innovative Research Team in University (Grant No. IRT1221), the Hong Kong Scholars Program, the Shanghai Leading Academic Discipline Project (Grant No. B603), and the Program of Introducing Talents of Discipline to Universities (No. 111-2-04).

## Notes and references

<sup>a</sup> State Key Laboratory for Modification of Chemical Fibers and Polymer Materials, College of Materials Science and Engineering, Donghua University, Shanghai 201620, China

<sup>b</sup> School of material engineering, Shanghai university of engineering science, Shanghai 201620, China

† Electronic Supplementary Information (ESI) available: [The Low-magnification SEM image of the as-prepared high yield product (Fig. S1)]. See DOI: 10.1039/b000000x/

- X. X. Xu, J. Zhang and X. Wang, *J. Am. Chem. Soc.*, 2008, **130**, 12527.
- X. G. Han, M. S. Jin, S. F. Xie, Q. Kuang, Z. Y. Jiang, Y. Q. Jiang, Z. X. Xie and L. S. Zheng, *Angew. Chem. Int. Ed.*, 2009, **48**, 9180.
- D. F. Zhang, L. D. Sun, J. L. Yin and C. H. Yan, *Adv. Mater.*, 2003, **15**, 1022.
- Y. L. Wang, X. C. Jiang and Y. N. Xia, *J. Am. Chem. Soc.*, 2003, **125**, 16176.
- Y. Wang, H. C. Zeng and J. Y. Lee, *Adv. Mater.*, 2006, **18**, 645.
- J. S. Chen and X. W. Lou, *Mater. Today*, 2012, **15**, 246.
- J. P. Liu, Y. Y. Li, X. T. Huang, R. M. Ding, Y. Y. Hu, J. Jiang and L. Liao, *J. Mater. Chem.*, 2009, **19**, 1859.
- Z. Y. Zhang, R. J. Zou, G. S. Song, L. Yu, Z. G. Chen and J. Q. Hu, *J. Mater. Chem.*, 2011, **21**, 17360.
- H. K. Wang and A. L. Rogach, *Chem. Mater.*, 2014, **26**, 123.
- Y. Liu, Y. Jiao, Z. L. Zhang, F. Y. Qu, A. Umar and X. Wu, *ACS Appl. Mater. Interfaces*, 2014, **6**, 2174.
- S. J. Han, B. C. Jang, T. Kim and S. M. Oh, *Adv. Funct. Mater.*, 2005, **15**, 1845.
- H. Kim and J. Cho, *J. Mater. Chem.*, 2008, **18**, 771.
- J. S. Chen and X. W. Lou, *Small*, 2013, **9**, 1877.
- L. N. Gao, F. Y. Qu and X. Wu, *J. Mater. Chem. A*, 2014, **2**, 7367.
- R. J. Zou, J. Q. Hu, Z. Y. Zhang, Z. G. Chen and M. Y. Liao, *CrystEngComm*, 2011, **13**, 2289.
- H. He, T. H. Wu, C. L. Hsin, K. M. Li, L. J. Chen, Y. L. Chueh, L. J. Chou and Z. L. Wang, *Small*, 2006, **2**, 116.

- 17 H. J. Snaith and C. Ducati, *Nano Lett.*, 2010, **14**, 1259.
- 18 M. A. Hossain, J. R. Jennings, Z.Y. Koh and Q. Wang, *ACS Nano*, 2011, **5**, 3172.
- 19 Y. T. Han, X. Wu, Y. L. Ma, L. H. Gong, F. Y. Qu and H. J. Fan, *CrystEngComm*, 2011, **13**, 3506.
- 20 B. X. Jia, W. N. Jia, F. Y. Qu and X. Wu, *RSC Adv.*, 2013, **3**, 12140.
- 21 J. Huang and Q. Wan, *Sensors*, 2009, **9**, 9903.
- 22 K. J. Choi and H. W. Jang, *Sensors*, 2010, **10**, 4083.
- 23 H. K. Wang, F. Fu, F. H. Zhang, H. E. Wang, S. V. Kershaw, J. Q. Xu, S. G. Sun and A. L. Rogach, *J. Mater. Chem.*, 2012, **22**, 2140.
- 24 R. McCormack, N. Shirato, U. Singh, S. Das, A. Kumar, H. J. Cho, R. Kalyanaraman and S. Seal, *Nanoscale*, 2012, **4**, 7256.
- 25 Y. Liu and M. Liu, *Adv. Funct. Mater.*, 2005, **15**, 57.
- 26 J. Pan, H. Shen, U. Werner, J. D. Prades, F. H. Ramirez, F. Soldera, F. Mucklich and S. Mathur, *J. Phys. Chem. C*, 2011, **115**, 15191.
- 27 D. W. Chu, Y. Masuda, T. Ohji and K. Kato, *Chem. Engn. J.*, 2011, **168**, 955.
- 28 X. B. Li, X. W. Wang, Q. Shen, J. Zheng, W. H. Liu, H. Zhao, F. Yang and H. Q. Yang, *ACS Appl. Mater. Interfaces*, 2013, **5**, 3033.
- 29 S. Chen, M. Wang, J. F. Ye, J. G. Cai, Y. R. Ma, H. H. Zhou and L. M. Qi, *Nano Res.*, 2013, **6**, 243.
- 30 G. X. Cheng and C. Liu, *Mater. Chem. Phys.*, 2002, **77**, 359.
- 31 M. H. Huang, B. S. Dunn and J. I. Zink, *J. Am. Chem. Soc.*, 2000, **122**, 3739.
- 32 H. Kunieda, N. Kanei, I. Tobita, K. Khara and A. Yuki, *Colloid Polym. Sci.*, 1995, **273**, 584.
- 33 Y. Tan, C. C. Li, Y. Wang, J. F. Tang and X. C. Ouyang, *Thin Solid Films*, 2008, **516**, 7840.
- 34 Y. J. Chen, X. Y. Xue, Y. G. Wang and T. H. Wang, *Appl. Phys. Lett.*, 2005, **87**, 233503.
- 35 M. H. Xu, F. S. Cai, J. Yin, Z. H. Yuan and L. J. Bie, *Sens. Actuators, B*, 2010, **145**, 875.
- 36 K. M. Li, Y. J. Li, M. Y. Lu, C. Kuo and L. J. Chen, *Adv. Funct. Mater.*, 2009, **19**, 2453.
- 37 J. P. Ge, J. Wang, H. X. Zhang, X. Wang, Q. Peng and Y. D. Li, *Sens. Actuators, B*, 2006, **113**, 937.
- 38 M. M. Rahman, A. Jamal, S. B. Khan and M. Faisal, *Biosens. Bioelectron.*, 2011, **28**, 127.

## Graphic abstract

3D hierarchical SnO<sub>2</sub> nanorods array on homogeneous substrate was prepared by one-step solvothermal route and exhibited high response to ethanol gas.

